Journal of Dental Sciences

Volume 21 | Issue 2 Article 38

2026

Development and characterization of an exosome-loaded biomimetic hydroxyapatite/gelatin scaffold for enhanced dental pulp regeneration

Yuen-Shan Tsai

Shih-Jung Cheng

Tsao-Li Chuang

Shu-Fang Chang

Chun-Pin Lin

Available online at https://jds.ads.org.tw/journal/

Digital Commons

journal homepage: https://jds.ads.org.tw/journal/

Original Article

Development and characterization of an exosome-loaded biomimetic hydroxyapatite/gelatin scaffold for enhanced dental pulp regeneration

Yuen-Shan Tsai [a], Shih-Jung Cheng [b,c], Tsao-Li Chuang [b], Shu-Fang Chang [d], Feng-Huei Lin [e,f], Chun-Pin Lin [b,c,g*]

[a] *Graduate Institute of Oral Biology, School of Dentistry, National Taiwan University, Taipei, Taiwan*
[b] *Graduate Institute of Clinical Dentistry, School of Dentistry, National Taiwan University, Taipei, Taiwan*
[c] *Department of Dentistry, National Taiwan University Hospital, Taipei, Taiwan*
[d] *Department of Dentistry, Shin Kong Wu Ho-Su Memorial Hospital, Taipei, Taiwan*
[e] *Institute of Biomedical Engineering, College of Medicine and College of Engineering, National Taiwan University, Taipei, Taiwan*
[f] *Institute of Biomedical Engineering and Nanomedicine, National Health Research Institutes, Miaoli, Taiwan*
[g] *School of Dentistry, College of Dental Medicine, Kaohsiung Medical University, Kaohsiung, Taiwan*

Received 19 November 2025; Final revision received 19 November 2025
Available online 1 April 2026

KEYWORDS
Exosomes;
Dental pulp stem cells;
Hydroxyapatites;
Gelatin;
Tissue regeneration;
Endodontics

Abstract *Background/purpose:* Regenerative endodontic procedures aim to biologically restore the dentin–pulp complex. Exosomes derived from dental pulp stem cells (D-Exo) have emerged as promising acellular therapeutic agents due to their ability to modulate the regenerative microenvironment. This study evaluated the regenerative potential of D-Exo–loaded hydroxyapatite/gelatin (HAp/Gel) scaffolds in dentin–pulp complex regeneration.
Materials and methods: A biomimetic HAp/Gel scaffold was fabricated and characterized for morphology, swelling behavior, degradation, and cytocompatibility. D-Exo were isolated from dental pulp stem cells (DPSCs) and analyzed using transmission electron microscopy (TEM), nanoparticle tracking analysis, and western blotting. Their effects on DPSC proliferation were examined *in vitro*. *In vivo* regenerative efficacy was assessed using a rat molar pulp exposure model, followed by micro–computed tomography (μ-CT) at 2 and 4 weeks.

* Corresponding author. Department of Dentistry, National Taiwan University Hospital, No. 1, Changde Street, Zhongzheng District, Taipei 100229, Taiwan.
E-mail address: chunpinlin@gmail.com (C.-P. Lin).

https://doi.org/10.1016/j.jds.2025.11.017

Results: The HAp/Gel scaffold exhibited an interconnected porous architecture, controlled degradation, and excellent cytocompatibility. Isolated D-Exo displayed typical vesicular morphology (approximately 117 nm) and expressed CD9, CD63, and CD81. D-Exo enhanced DPSC proliferation in a dose-dependent manner. μ-CT analysis revealed early mineralized tissue formation at 2 weeks and dentin bridge formation at 4 weeks, with more extensive mineralized deposition in the D-Exo—loaded HAp/Gel scaffold group.
Conclusion: The D-Exo—loaded HAp/Gel scaffold demonstrated favorable biocompatibility and enhanced dentin—pulp complex regeneration *in vivo*. This biomimetic acellular approach may serve as a promising strategy for future regenerative endodontic applications.

Introduction

Dental pulp is essential for maintaining tooth vitality, providing sensory function, and supporting dentin formation and repair.[1,2] However, when pulp tissue becomes exposed due to caries or trauma, inflammation and necrosis often ensue, ultimately leading to periapical pathology and tooth loss.[3,4] Conventional root canal therapy (RCT) effectively eradicates infection and preserves the tooth structure, yet it removes all vital tissue within the canal system, leaving the tooth devitalized, more brittle, and devoid of sensory function.[5]

To address these limitations, regenerative endodontic procedures (REPs) have been introduced as biologically based treatments that aim to restore functional pulp—dentin complex vitality rather than simply replacing lost tissue with inert filling materials.[6–8] According to the American Association of Endodontists (AAE) clinical considerations, REPs utilize the triad of tissue engineering—stem cells, signaling molecules, and scaffold materials—to promote the regeneration of vascularized, innervated tissue within the root canal space.[9] Despite the encouraging outcomes reported in immature teeth, the predictability and quality of regenerated tissues remain variable, underscoring the need for improved biomaterials capable of creating a more favorable microenvironment for regeneration.[10–12]

Dental pulp stem cells (DPSCs) play a pivotal role in this process due to their capacity for self-renewal, multilineage differentiation, and secretion of trophic factors that stimulate angiogenesis and dentinogenesis.[13,14] Increasing evidence suggests that the regenerative effects of DPSCs are largely mediated through exosomes, nanosized extracellular vesicles that facilitate intercellular communication by transferring bioactive molecules such as proteins, lipids, and microRNAs. DPSC-derived exosomes (D-Exo) have demonstrated the ability to enhance odontoblastic differentiation, modulate inflammation, and promote neovascularization.[15–17] However, their clinical utility remains limited by short half-life, rapid degradation, and challenges in achieving localized, sustained delivery.[18]

To overcome these limitations, biomimetic scaffold systems have been developed to provide both mechanical support and biological cues for endodontic regeneration.[19–22] Among these, hydroxyapatite (HAp) and gelatin (Gel) composites have garnered significant interest.[23–25] HAp, the principal inorganic component of dentin and bone, offers excellent biocompatibility and osteoconductivity, while gelatin, derived from partially hydrolyzed collagen, mimics the extracellular matrix (ECM) to support cell adhesion and proliferation. A composite HAp/Gel scaffold combines these advantages, creating a bioactive, degradable, and clinically manageable platform that can also serve as a carrier for bioactive agents.[26–28]

In this study, we developed an exosome-loaded HAp/Gel biomimetic scaffold and evaluated its potential to promote dental pulp regeneration. We hypothesized that the synergistic combination of DPSC-derived exosomes and a bioactive HAp/Gel scaffold could enhance odontogenic differentiation, angiogenesis, and tissue organization—offering a novel acellular approach that aligns with the clinical objectives of regenerative endodontic procedures and represents a translational step toward next-generation biologically based endodontic therapies.

Materials and methods

HAp/gel scaffold fabrication

Preparation of HAp powder

Hydroxyapatite powder was synthesized using the coprecipitation method. Briefly, calcium hydroxide powder was dissolved in deionized water and stirred continuously at 85 °C until fully dissolved. Subsequently, 0.3 M phosphoric acid solution was slowly added dropwise into 0.5 M calcium hydroxide solution under constant stirring to ensure homogeneous mixing. The pH of the reaction mixture was adjusted to the desired range, and the solution was stirred for 2 h, followed by standing for 20 h to allow complete precipitation. The resulting precipitate was collected by centrifugation at 10,000 rpm for 10 min and washed three times with deionized water to remove impurities. The final product was freeze-dried and stored for further use (Fig. 1A).

Preparation of HAp/Gel scaffold

Gelatin powder was dissolved in deionized water (ddH_2O) under constant stirring at 40 °C for 45 min to prepare a 10 % (w/v, 100 mg/mL) gelatin solution. Then, 2.1 g of HAp powder was added to the gelatin solution and stirred continuously until a uniform suspension was obtained. The

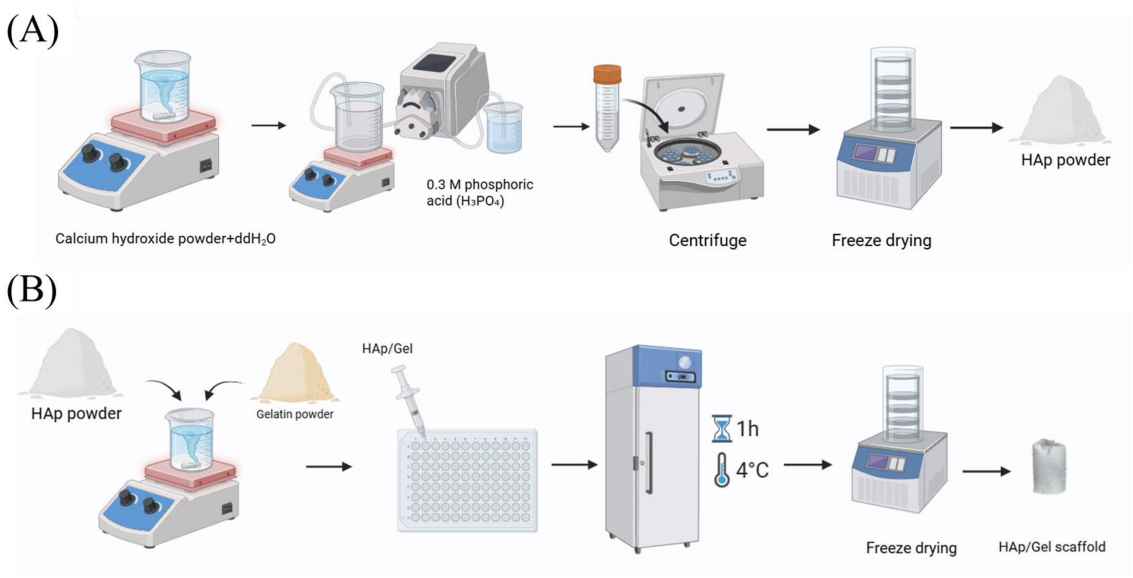

Figure 1 Illustrates the preparation process. (A) Hydroxyapatite (HAp) powder.; (B) HAp/Gel scaffold fabrication.

mixed solution was poured into 96-well culture plates and kept at 4 °C for 1 h to allow gelation, forming the HAp/Gel scaffold. The scaffolds were subsequently freeze-dried to obtain a stable porous structure and stored in a desiccator for further experiments (Fig. 1B).

Dental pulp stem cell (DPSC) culture and exosome isolation

Ethical approval

This study was approved by the Research Ethics Committee A of National Taiwan University Hospital (IRB No. 202501089RINA), and written informed consents were obtained from all donors.

Cell culture

Human dental pulp stem cells (DPSCs, passage 5) were isolated from extracted sound teeth and cryopreserved in liquid nitrogen until use. For culture, frozen DPSC vials were rapidly thawed in a 37 °C water bath, followed by centrifugation at 400×*g* for 5 min to remove the DMSO-containing cryoprotectant. The cell pellet was resuspended in fresh culture medium consisting of Dulbecco's Modified Eagle Medium (DMEM) supplemented with 10 % fetal bovine serum (FBS), 1 % non-essential amino acids (NEAA), and 1 % penicillin–streptomycin. Approximately 4×10^5 cells were seeded into 10-cm culture dishes and maintained at 37 °C in a humidified incubator with 5 % CO_2. Cell morphology and confluence were monitored using an inverted phase-contrast microscope.

Exosome production and isolation

DPSCs (4×10^5 cells) were seeded in 10-cm culture dishes and cultured until reaching 80–90 % confluence. The cells were washed three times with phosphate-buffered saline (PBS) and then incubated with DMEM supplemented with 10 % exosome-depleted FBS for 48 h. The conditioned medium (approximately 40 mL) was collected for exosome purification. Exosomes were isolated using the qEVoriginal Gen 2 column (70 nm, IZON Science) according to the manufacturer's instructions. The collected eluates were centrifuged at 3,000×*g* for 10 min, and the supernatant was filtered through a 0.22 μm syringe filter. The exosome suspension was further concentrated using Amicon® Ultra centrifugal filters (100 kDa, Millipore) to a final volume of 0.5 mL. Exosomes were quantified based on protein concentration using the Qubit 4.0 fluorometer (Thermo Fisher Scientific, Waltham, MA, USA) and stored at −80 °C for subsequent experiments.

Exosome characterization

The morphology of DPSC-derived exosomes (D-Exo) was examined by transmission electron microscopy (TEM). Particle size distribution and concentration were measured using nanoparticle tracking analysis (NTA). The presence of exosomal marker proteins CD63, CD81, and Alix was confirmed by Western blot analysis.

Characterization of the HAp/Gel scaffold

Fourier transform infrared spectroscopy (FTIR)

The chemical structure of the fabricated scaffolds was analyzed using an attenuated total reflectance Fourier transform infrared spectrometer (ATR-FTIR; Vertex 80v, Bruker, Germany) over the wavenumber range of 500–4000 cm^{-1} with a resolution of 4 cm^{-1}. Characteristic absorption peaks were identified to determine functional groups and bonding interactions between HAp and gelatin.

Scanning electron microscopy (SEM)

The surface morphology and microstructure of the scaffolds were observed using a field-emission scanning electron microscope (FE-SEM; JSM-7001F, JEOL, Tokyo, Japan). Prior to imaging, the samples were sputter-coated with gold to enhance conductivity and image quality.

Degradation and swelling behavior of the scaffolds

Degradation test

To evaluate degradation behavior, HAp/Gel scaffolds were immersed in 1 × PBS (pH 7.4) at 37 °C and retrieved at predetermined time intervals (0, 6, 12, 24, 30, 36, 72, 78, 108, 120, 126, 132, 144, and 150 h). At each time point, the samples were gently removed, blotted with filter paper to eliminate excess surface water, and weighed (Wt).

The degradation rate was calculated using the following equation:

$$\text{Degradation rate } (\%) = \frac{W_0 - W_t}{W_0} \times 100$$

where W_0 represents the initial weight of the hydrated sample and Wt is the sample weight at each time point.

Swelling test

For swelling measurements, scaffolds were immersed in 1 × PBS at 37 °C and collected at time intervals of 0, 2, 3, 6, 9, and 12 h. The samples were blotted with filter paper and weighed immediately (Wt).

The swelling ratio was calculated as follows:

$$\text{Swelling ratio } (\%) = \frac{W_t - W_d}{W_d} \times 100$$

where Wd represents the initial dry weight and Wt is the wet weight at each specific time point.

These measurements were conducted to assess the degradation profile, water uptake capacity, and structural stability of the scaffolds under physiological conditions.

In vitro studies: cytocompatibility evaluation

Preparation of extracts from scaffolds

The extraction medium of each HAp/Gel scaffold was prepared according to the ISO 10993-12 standard. Briefly, 0.8 g of freeze-dried scaffold was sterilized under ultraviolet (UV) light for 15 min and immersed in 4 mL of Eagle's Minimum Essential Medium (EMEM) supplemented with 10 % fetal bovine serum (FBS) and 1 % penicillin—streptomycin. The samples were incubated at 37 °C for 24 h. After incubation, the extracts were centrifuged at 11,000 rpm for 10 min, and the supernatant was filtered through a 0.22 μm membrane filter to obtain the final extract with a concentration of 0.2 g/mL. Negative control (Al_2O_3) and positive control (zinc diethyldithiocarbamate, ZDEC) extracts were prepared in the same manner.

Cell culture

Mouse fibroblast cell line L929 was used for cytocompatibility testing. Cells were cultured in EMEM containing 10 % FBS and 1 % penicillin—streptomycin at 37 °C in a humidified incubator with 5 % CO_2.

WST-1 cell viability assay

L929 cells were seeded into 96-well culture plates at a density of 1.0 × 10^4 cells/well in 200 μL of medium and incubated for 24 h. The culture medium was then replaced with the respective scaffold extracts, and the cells were further incubated for 24 h. Subsequently, WST-1 reagent (diluted 1:10, Roche Diagnostics, Rotkreuz, Switzerland) was added to each well and incubated for 4 h. The absorbance was measured at 450 nm using a microplate reader.

Cell viability was calculated according to the following formula:

$$\text{Viability } (\%) = \frac{OD_{test} - OD_{blank}}{OD_{control} - OD_{blank}} \times 100\%$$

Live/dead cell staining

For morphological observation of viable and dead cells, L929 cells were seeded in 35 mm culture dishes at a density of 1.0 × 10^5 cells/mL and incubated for 24 h. The culture medium was replaced with each group's extract, including the control, negative control, positive control, and HAp/Gel scaffold extract. After 24 h of incubation, the cells were stained using a Live/Dead staining kit (Thermo Fisher Scientific) and incubated at room temperature in the dark for 30 min. The stained cells were washed with PBS and observed using a fluorescence microscope (Nikon, Tokyo, Japan) to assess cell viability and morphology.

Loading of exosomes onto HAp/Gel scaffolds

Freeze-dried HAp/Gel scaffolds were sterilized and immersed in phosphate-buffered saline containing D-Exo (100 μg/mL). The samples were incubated at 4 °C for 12 h to facilitate exosome adsorption onto the scaffold surface. After incubation, the scaffolds were gently rinsed with PBS to remove unbound exosomes and stored at 4 °C until further use in subsequent assays.

In vivo evaluation of dentin—pulp complex regeneration

All animal procedures were approved by the Institutional Animal Care and Use Committee of National Taiwan University (NTU IACUC No. 20230509) and conducted in accordance with the NTU Guidelines for the Care and Use of Laboratory Animals. Twelve-week-old male Wistar rats were used as the experimental model. Maxillary molars were selected for testing, with observation endpoints at 2 and 4 weeks postoperatively.

Surgical procedure

Rats were anesthetized by intramuscular injection of Zoletil 50 (20 mg/kg). After disinfection with 0.2 % chlorhexidine gluconate, a Class I cavity was prepared on the occlusal surface using a high-speed handpiece with a round diamond bur under saline irrigation. Following hemostasis, the test material was applied to the exposed pulp and covered with glass ionomer cement for coronal sealing (see Fig. 2).

Micro—computed tomography (μ-CT) analysis

After sacrifice at 2 and 4 weeks, the specimens were fixed in formalin for 10 days and subsequently scanned using μ-CT to facilitate comprehensive, nondestructive evaluation of

the samples. Data visualization and 3D reconstruction were performed using DataViewer and CTVox software.

Statistical analysis

All quantitative data were expressed as mean ± standard error of the mean (SEM). Statistical analyses were performed using SPSS 18.0 software (SPSS Inc., Chicago, IL, USA). One-way analysis of variance (ANOVA) followed by Student's t-test for pairwise comparisons was used to evaluate statistical differences. A *P*-value of less than 0.05 was considered statistically significant.

Results

Fabrication of HAp/Gel scaffolds

Hydroxyapatite powder was synthesized using a coprecipitation method with controlled crystal morphology and particle size (Fig. 3A). The synthesized HAp was then blended with gelatin to fabricate a composite scaffold. After thorough mixing, the HAp/Gel mixture was cast into molds and allowed to gel at 4 °C, forming a three-dimensional porous scaffold (Fig. 3B).

This fabrication approach yielded HAp/Gel scaffolds with well-defined morphology and promising potential for biological applications.

Surface morphology of HAp/Gel scaffolds

The surface morphology of the HAp/Gel scaffolds was examined using SEM. As shown in Fig. 4, the scaffolds exhibited a highly porous three-dimensional structure with pore sizes ranging from several tens to several hundred micrometers. The internal pore walls displayed a rough and irregular texture, which may be attributed to the homogeneous dispersion of HAp particles within the gelatin matrix.

Such an interconnected porous architecture increases the specific surface area of the scaffold and provides a favorable microenvironment for cell adhesion and growth.

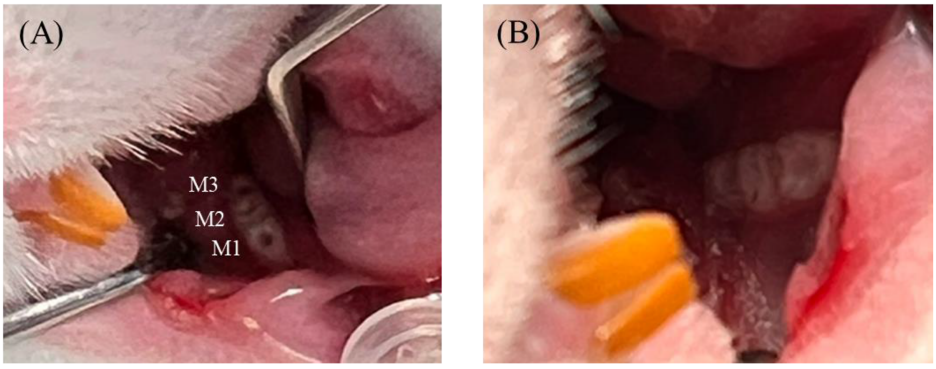

Figure 2 Access preparation and coronal sealing. (A) Access opening prepared to expose the maxillary molar pulp (M1–M3 labeled). (B) Final coronal sealing after placement of the scaffold material in the pulp exposure cavity.

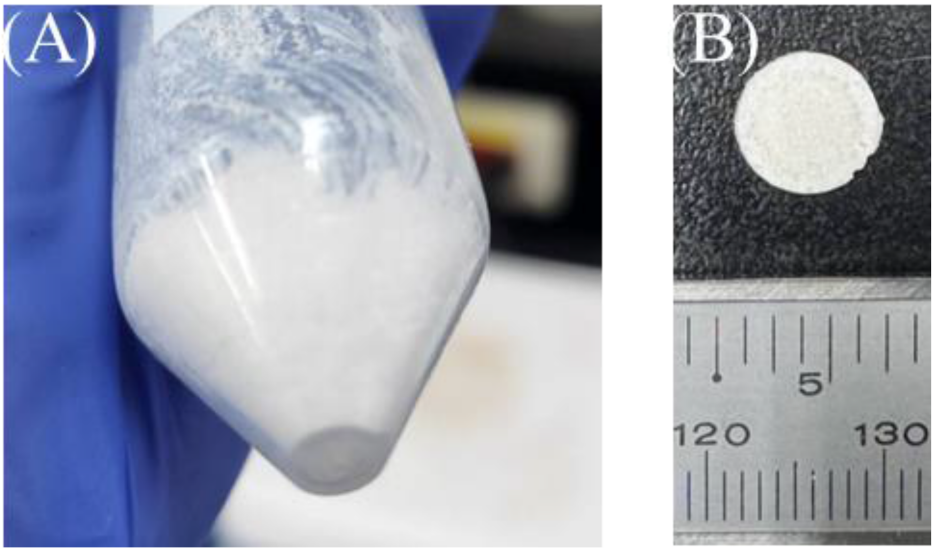

Figure 3 Fabrication and appearance of hydroxyapatite/gelatin (HAp/Gel) scaffolds. (A) Hydroxyapatite (HAp) powder; (B) HAp/Gel scaffold.

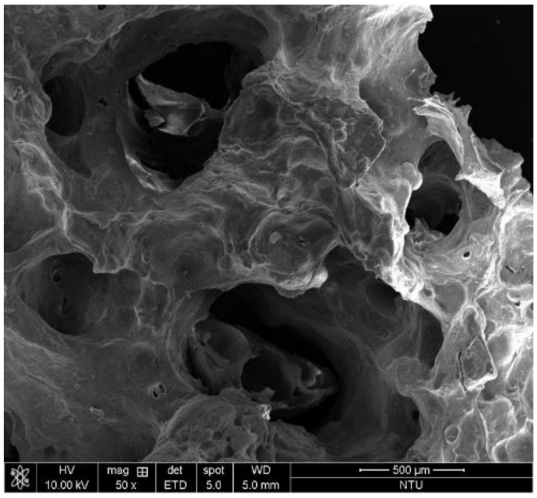

Figure 4 Scanning electron microscopy (SEM) image of the hydroxyapatite/gelatin (HAp/Gel) scaffold. The scaffold shows a highly porous, interconnected three-dimensional structure with rough internal surfaces. Scale bar = 500 μm.

Fourier transform infrared (FTIR) spectroscopic analysis

The FTIR spectra of the HAp/Gel scaffolds revealed characteristic absorption peaks corresponding to both hydroxyapatite and gelatin components (Fig. 5). Distinct P—O—P bending vibration peaks were observed at approximately 560 and 600 cm^{-1}, representing the typical phosphate group signals of hydroxyapatite. In addition, a prominent P—O stretching vibration peak appeared near 1040 cm^{-1}, further confirming the presence of phosphate groups within the scaffold matrix.

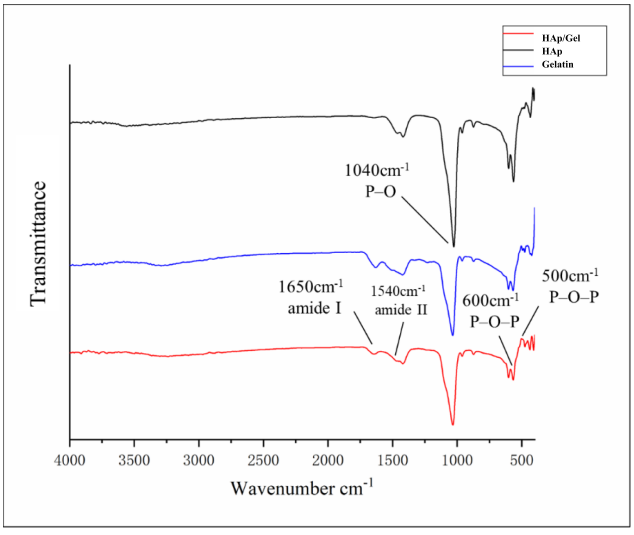

Figure 5 Fourier transform infrared (FTIR) spectra of hydroxyapatite (HAp), gelatin (Gel), and HAp/Gel scaffolds. Characteristic absorption peaks of phosphate groups from HAp (≈560, 600, and 1040 cm^{-1}) and amide bands from gelatin (1650 and 1540 cm^{-1}) confirm successful composite formation.

Moreover, the absorption bands detected at 1650 cm^{-1} (amide I) and 1540 cm^{-1} (amide II) were attributed to the characteristic amide vibrations of gelatin, indicating the successful incorporation of gelatin into the composite structure. The coexistence of these peaks suggests the formation of a stable molecular interaction between HAp and gelatin within the scaffold.

Degradation behavior of HAp/Gel scaffolds

The structural stability of the HAp/Gel scaffold was evaluated under physiological conditions in PBS. As shown in Fig. 6, the scaffold exhibited a rapid initial degradation profile. After 6 h of immersion, the remaining weight was approximately 86.7 % ± 4.8 %, which decreased to 70.8 % ± 6.1 % at 12 h, and further declined to 25.1 % after 24 h (see Fig. 7).

By 150 h, only about 5.7 % of the scaffold structure remained, indicating its fast-degrading characteristics. This degradation behavior suggests that the HAp/Gel scaffold is suitable for short-term structural support during the early stages of tissue regeneration.

Swelling behavior of HAp/Gel scaffolds

The swelling properties of the HAp/Gel scaffolds were evaluated in PBS to assess their water absorption capacity. As shown in Fig. 8, the scaffolds rapidly absorbed water during the initial immersion period, reaching a swelling ratio of approximately 200 % after 2 h. The swelling ratio continued to increase gradually and reached about 280 % at 12 h.

This rapid and sustained swelling behavior indicates that the HAp/Gel scaffolds possess excellent hydrophilicity, which may facilitate nutrient diffusion and cell infiltration during tissue regeneration.

WST-1 cell viability assay

The cytocompatibility of the fabricated scaffolds was evaluated using the WST-1 assay. As shown in Fig. 9, the positive control group (zinc diethyldithiocarbamate, ZDEC) exhibited almost no cell viability, confirming the sensitivity and reliability of the assay for detecting cytotoxicity. In contrast, the negative control group (Al_2O_3) demonstrated a high cell viability of 94.1 ± 0.3 %, comparable to that of the untreated control, indicating the stability and reproducibility of the testing procedure.

Notably, the HAp/Gel scaffold exhibited excellent biocompatibility, with a cell viability of 91.5 ± 0.3 %, which is well above the 80 % cytocompatibility threshold defined by ISO 10993-5. These results indicate that the developed scaffold does not exert significant cytotoxic effects and is suitable for further biological applications.

Live/dead cell staining

To further evaluate the cytocompatibility of the tested materials, a Live/Dead staining assay was performed (green fluorescence indicates viable cells; red fluorescence indicates dead cells; scale bar = 100 μm). As shown in

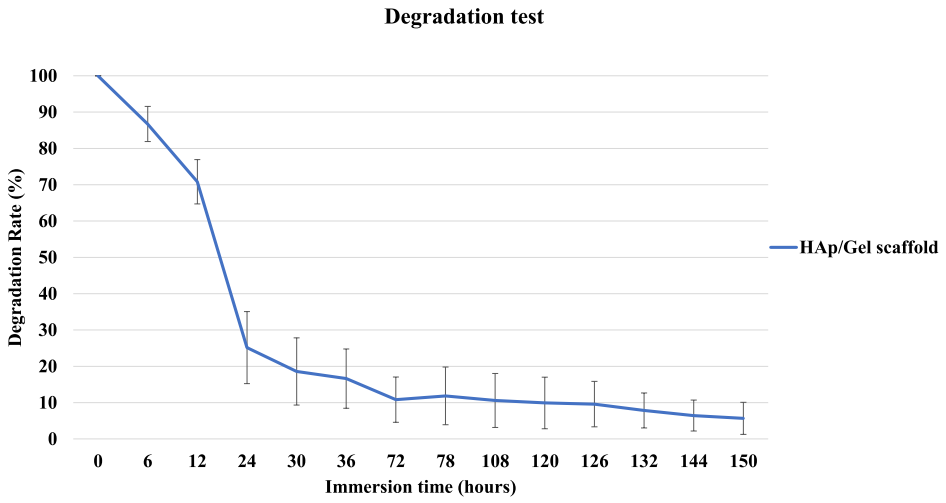

Figure 6 Degradation profile of hydroxyapatite/gelatin (HAp/Gel) scaffolds. The HAp/Gel scaffold exhibited a rapid degradation rate during the first 24 h, followed by a gradual decrease in weight over 150 h of immersion in PBS.

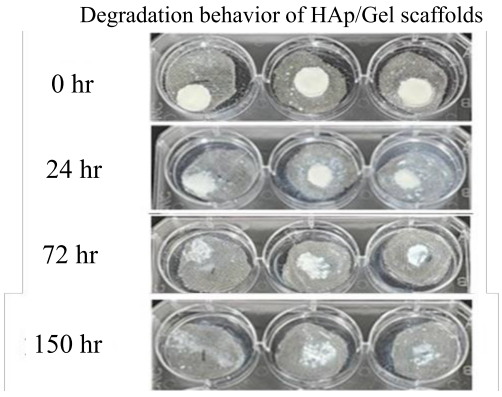

Figure 7 Visual observation of hydroxyapatite/gelatin (HAp/Gel) scaffold degradation.

Fig. 10, cells in the positive control group exhibited predominantly red fluorescence, indicating extensive cell death. In contrast, the negative control group and the HAp/Gel scaffold group displayed widespread green fluorescence with minimal red signal, demonstrating excellent cell viability and confirming the good biocompatibility of the developed scaffold.

Isolation and morphological characterization of DPSC-derived exosomes

Dental pulp stem cells (DPSCs; 4×10^5 cells per 10-cm dish) were seeded and cultured at 37 °C until reaching approximately 80–90 % confluence. The culture medium was then removed, and the cells were washed three times with PBS to eliminate residual serum components. The cells were subsequently incubated in DMEM supplemented with 10 % exosome-depleted FBS for 48 h, after which the conditioned medium was collected.

A total of 40 mL of conditioned medium was subjected to exosome isolation using qEVoriginal Gen 2 size-exclusion chromatography columns (70 nm, Izon Science, Medford, MA, USA) following the manufacturer's instructions.

TEM demonstrated that the isolated exosome exhibited the typical oval morphology with a bilayer membrane

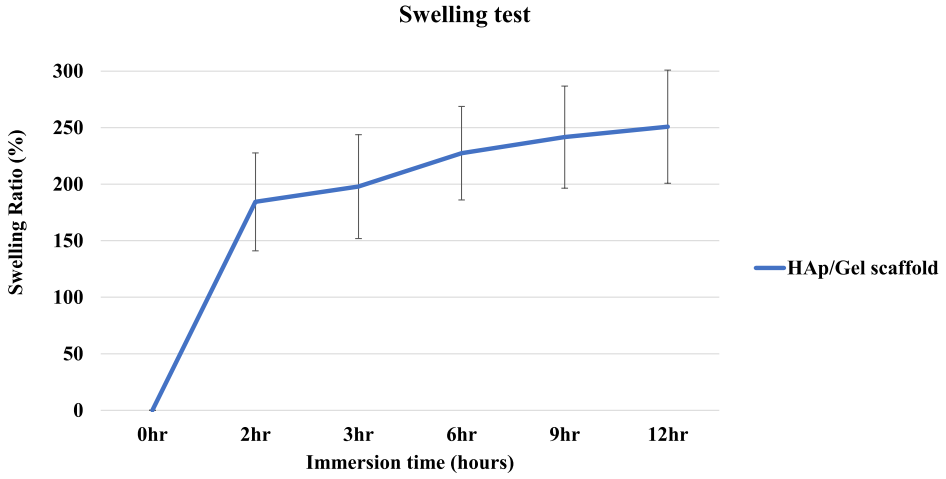

Figure 8 Swelling behavior of hydroxyapatite/gelatin (HAp/Gel) scaffolds. The scaffolds rapidly absorbed water within the first 2 h, reaching a swelling ratio of approximately 200 %, and gradually increased to about 280 % after 12 h of immersion in PBS.

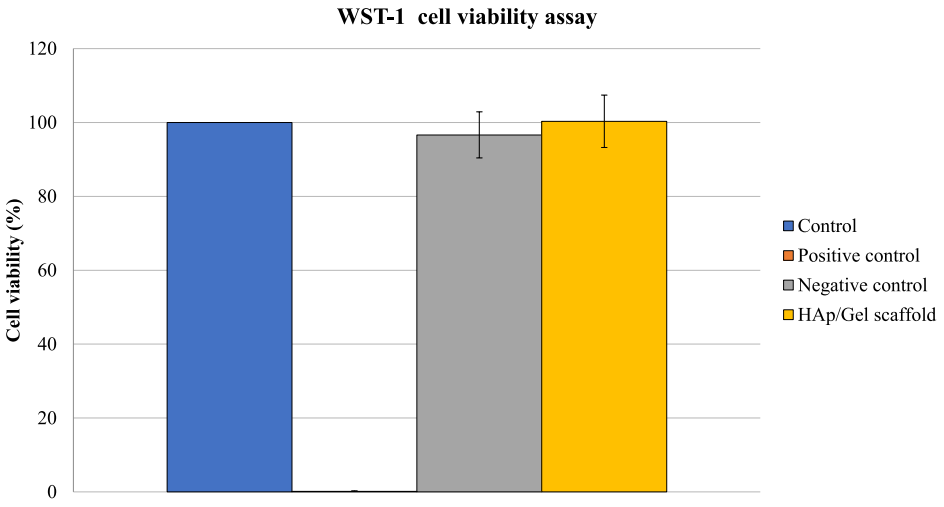

Figure 9 Cell viability of L929 fibroblasts cultured with hydroxyapatite/gelatin (HAp/Gel) scaffold extracts.

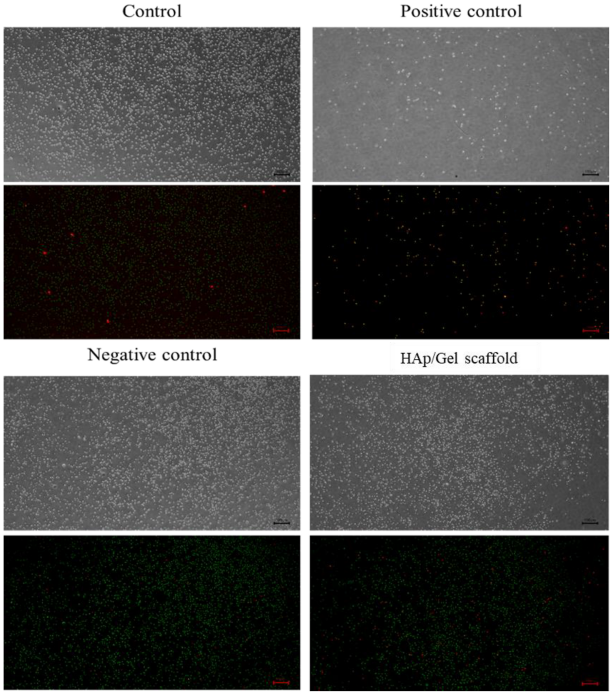

Figure 10 Live/Dead fluorescence images of L929 fibroblasts cultured with hydroxyapatite/gelatin (HAp/Gel) scaffold extracts (scale bar = 100 μm). Green fluorescence indicates viable cells, and red fluorescence indicates dead cells. The HAp/Gel scaffold and negative control groups showed predominantly green fluorescence, while the positive control exhibited extensive red fluorescence, confirming the excellent cytocompatibility of the scaffold.

characteristic of exosomes, confirming successful isolation of D-Exo (Fig. 11).

Size distribution and concentration analysis of DPSC-derived exosomes

The size distribution and concentration of purified D-Exo were analyzed using a nanoparticle tracking analysis (NTA) system (NanoSight NS300, Malvern Instruments, Worcestershire, UK). The exosome samples were diluted 10—100 times with sterile PBS prior to measurement to ensure optimal particle count.

As shown in Fig. 12, the D-Exo exhibited a homogeneous size distribution, with particle diameters ranging from 100 to 125 nm, and a mode size of approximately 117.1 nm. The concentration of exosomes after purification was determined to be ($1.15 \times 10^{10} \pm 1.84 \times 10^{8}$ particles/mL) (mean ± SEM), consistent with the expected size and concentration range of typical exosome.

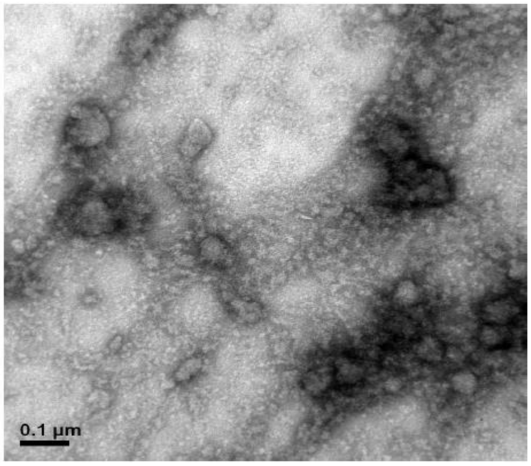

Figure 11 Transmission electron microscopy (TEM) image of dental pulp stem cell (DPSC)-derived exosomes (scale bar = 0.1 μm). The isolated extracellular vesicles exhibited a typical oval, bilayered morphology, confirming the successful isolation of exosomes from dental pulp stem cells.

Characterization of DPSC-derived exosomes

To confirm the identity of the purified exosomes derived from DPSC, the expression of specific exosomal surface markers was analyzed by Western blotting. Total protein was extracted from lysed exosome preparations and

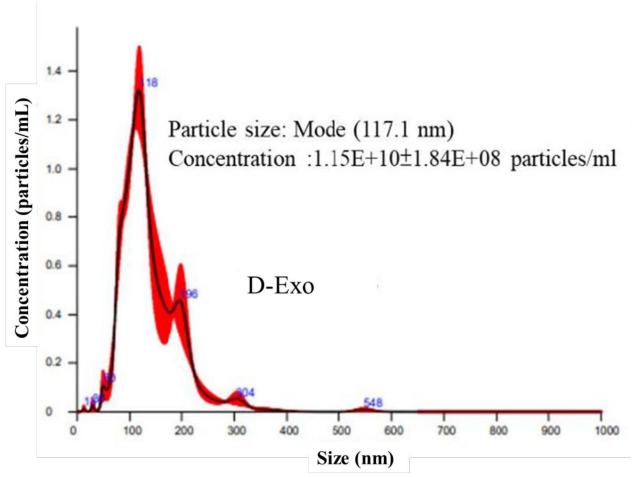

Figure 12 Characterization of dental pulp stem cell (DPSC)-derived exosomes by nanoparticle tracking analysis (NTA) and fluorescence imaging. NTA revealed that the DPSC-derived exosomes had a modal particle size of approximately 117.1 nm and a concentration of $1.15 \times 10^{10} \pm 1.84 \times 10^{8}$ particles/mL. Fluorescence imaging confirmed the presence of nanosized vesicles with uniform distribution, consistent with the typical size range of exosomes.

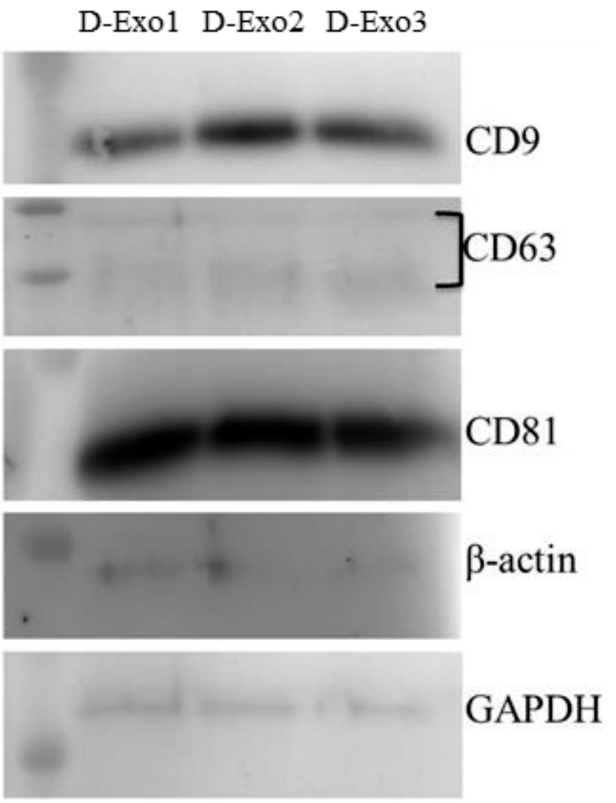

Figure 13 Western blot analysis of dental pulp stem cell (DPSC)-derived exosomes (D-Exo1–3). The isolated exosomes expressed characteristic markers CD9, CD63, and CD81, confirming the successful isolation of exosome from dental pulp stem cells. β-actin and GAPDH served as internal controls.

subjected to immunoblot analysis using antibodies against canonical exosomal markers.

As shown in Fig. 13, the presence of characteristic exosomal proteins CD9, CD63, and CD81 was clearly detected, confirming the successful isolation of DPSC-derived exosomes. These findings validate the purity and exosomal nature of the isolated vesicles.

Effects of DPSC-derived exosomes on cell proliferation

To evaluate the effect of purified exosomes on DPSC proliferation, cells were seeded in 96-well plates and treated with various concentrations of D-Exo. Cell proliferation was assessed at 1, 3, and 5 days using the CCK-8 assay.

As shown in Fig. 14A, after 24 h of treatment, cells exposed to D-Exo at a concentration of 10^{7} particles exhibited a significant increase in proliferation compared to the control group ($P < 0.05$). This proliferative effect became more pronounced at days 3 and 5 (Fig. 14B and C), indicating a time-dependent enhancement of cell growth.

These findings suggest that D-Exo promote DPSC proliferation in a dose-dependent manner, with an optimal effect observed at a cell-to-exosome ratio of approximately 1:1000 (cell: D-Exo). Data are presented as mean ± SEM, and statistical analysis was performed using Student's t-test ($P < 0.05$, $^{*}P < 0.01$).

In vivo evaluation of dentin–pulp complex regeneration by micro–CT

To evaluate the dentin–pulp regenerative potential of the HAp/Gel and HAp/Gel/D-Exo scaffolds, the materials were implanted into the molar pulps of Wistar rats. The animals were sacrificed at 2 and 4 weeks post-implantation for micro–computed tomography (μ-CT) analysis.

As shown in Fig. 15, color-coded μ-CT images revealed mineralized tissue deposition at 2 weeks (indicated by yellow arrows) in both groups; however, no apparent dentin bridge formation was observed at this stage. By 4 weeks, distinct dentin bridge formation was detected in both the HAp/Gel and HAp/Gel/D-Exo scaffold groups (red arrows). These findings suggest that both scaffolds promoted hard tissue formation, with D-Exo incorporation further enhancing dentin–pulp complex regeneration.

Discussion

In this study, a HAp/Gel scaffold incorporated with D-Exo was successfully fabricated and evaluated for its potential in dentin–pulp complex regeneration. Both hydroxyapatite and gelatin are widely used biomaterials with proven clinical safety. HAp, the principal inorganic component of dentin and bone, has long been applied in bone fillers and dental implant coatings owing to its excellent bioactivity and osteoconductivity. Gelatin, a natural derivative of collagen, provides high hydrophilicity, biodegradability, and cell adhesion sites, and is commonly used in medical dressings and tissue-engineered scaffolds. The

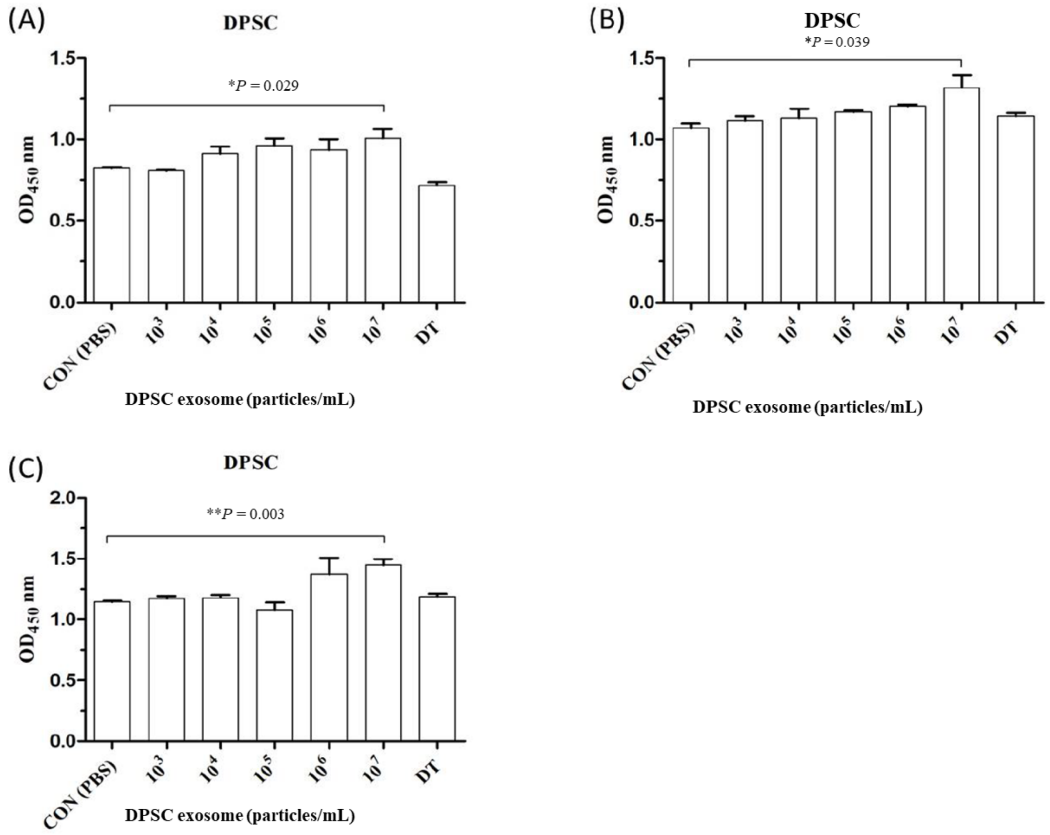

Figure 14 Cell proliferation of dental pulp stem cell (DPSC) treated with different concentrations of DPSC-derived exosomes (D-Exo). The CCK-8 assay was performed after 1 day (A), 3 days (B), and 5 days (C) of incubation. Treatment with D-Exo significantly enhanced DPSC proliferation in a dose-dependent manner, with the most pronounced effect observed at a concentration of 10^7 particles/mL ($P < 0.05$, $^*P < 0.01$).

combination of these two biomaterials yielded a three-dimensional porous scaffold with interconnected pores that facilitated cell attachment and nutrient exchange, while its controlled degradation provided initial mechanical support and allowed gradual tissue ingrowth. The results of WST-1 and Live/Dead assays demonstrated that the HAp/Gel scaffold exhibited excellent cytocompatibility, with cell viability exceeding the ISO 10993-5 threshold, confirming its biosafety and suitability as a regenerative scaffold.

The DPSC-derived exosomes isolated in this study displayed typical vesicular morphology, an average diameter of approximately 117 nm, and positive expression of exosomal markers CD9, CD63, and CD81. Functionally, D-Exo significantly promoted DPSC proliferation in a dose-dependent manner, particularly at a concentration of 10^7 particles/mL. Previous studies have shown that DPSC-derived exosomes contain multiple bioactive microRNAs—such as miR-27a, miR-140-5p, and miR-1246—that regulate odontogenic differentiation and angiogenesis via the Wnt/β-catenin, TGF-β/Smad, and PI3K/Akt signaling pathways. These findings are consistent with our results, suggesting that D-Exo acts as a potent biological regulator that enhances the regenerative capacity of the HAp/Gel scaffold.

In vivo micro—CT analysis further confirmed that both HAp/Gel and HAp/Gel/D-Exo scaffolds promoted mineralized tissue formation within the rat molar pulp cavity. Early mineral deposition was observed at 2 weeks, and distinct dentin bridge formation became evident by 4 weeks, with more extensive mineralized tissue detected in the D-Exo—incorporated group. These findings indicate that the addition of D-Exo effectively enhances dentin—pulp regeneration by stimulating cell—cell communication and biomineralization.

Nevertheless, this study had certain limitations. The small anatomical size of rat molars made it challenging to precisely locate the pulp exposure area during surgery, particularly in smaller animals, which may have introduced procedural variability. For future studies, the Lee—Song miniature pig model—which closely resembles human tooth anatomy and has been previously established by our team—could provide a more clinically relevant platform for evaluating pulp—dentin regeneration. In addition, only short-term (4-week) outcomes were assessed in this study, and the long-term stability and molecular mechanisms of exosome-mediated regeneration warrant further investigation.

In summary, the HAp/Gel/D-Exo scaffold developed in this study demonstrated favorable morphology, biosafety,

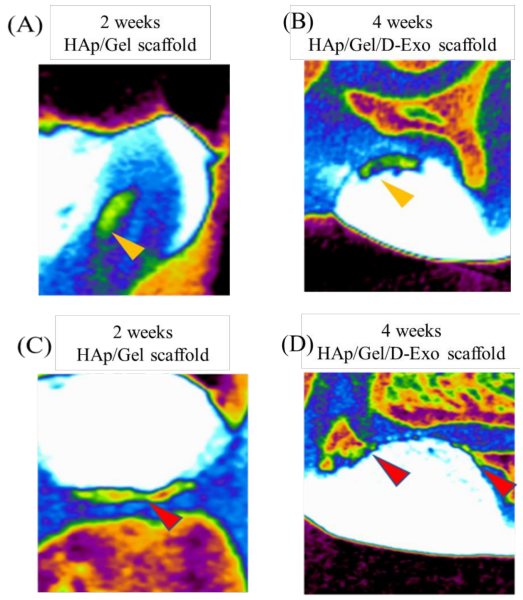

Figure 15 *In vivo* evaluation of dentin–pulp complex regeneration using micro–CT. (A) Hydroxyapatite/gelatin (HAp/Gel) (HG) group at 2 weeks showing initial mineralized tissue deposition (yellow arrow). (B) HAp/Gel/DPSC-derived exosomes HAp/Gel/D-Exo (HGE) group at 2 weeks demonstrating enhanced early mineralization (yellow arrow). (C) HG group at 4 weeks with evidence of dentin bridge formation (red arrow). (D) HGE group at 4 weeks showing more prominent and continuous dentin bridge formation (red arrow) compared with the HG group.

and biological functionality, effectively promoting dental pulp stem cell proliferation and dentin–pulp complex regeneration. These findings suggest that this biomimetic scaffold represents a promising candidate for future regenerative endodontic procedures and translational applications in clinical pulp regeneration.

This study successfully developed a HAp/Gel scaffold incorporated with dental pulp stem cell–derived exosomes for dentin–pulp complex regeneration. The composite scaffold exhibited favorable morphology, biodegradability, and excellent cytocompatibility, reflecting the intrinsic safety and clinical feasibility of both HAp and gelatin as biomaterials. The incorporation of D-Exo significantly enhanced DPSC proliferation and mineralization, likely through bioactive microRNAs and signaling pathways related to odontogenic differentiation. *In vivo* findings further demonstrated that the HAp/Gel/D-Exo scaffold effectively promoted mineralized tissue formation and dentin bridge development, confirming its regenerative potential.

Overall, the HAp/Gel/D-Exo scaffold represents a promising biomimetic platform that integrates structural support with biological regulation, offering a novel and clinically translatable approach for future regenerative endodontic procedures.

Declaration of competing interest

The authors have no conflicts of interest relevant to this article.

Acknowledgments

This research was supported by the National Science and Technology Council, Taiwan (Grant No. 114WFA0111241).

References

1. Huang GT. Dental pulp and dentin tissue engineering and regeneration–advancement and challenge. *Front Biosci (Elite Ed)* 2011;3:788–800.
2. Li XL, Fan W, Fan B. Dental pulp regeneration strategies: a review of status quo and recent advances. *Bioact Mater* 2024;38:258–75.
3. Hargreaves KM, Giesler T, Henry M, Wang Y. Regeneration potential of the young permanent tooth: what does the future hold? *Pediatr Dent* 2008;30:253–60.
4. Zhao Y, Fan W, Xu T, Tay F, Gutmann J, Fan B. Evaluation of several instrumentation techniques and irrigation methods on the percentage of untouched canal wall and accumulated dentine debris in c-shaped canals. *Int Endod J* 2019;52:1354–65.
5. Urkande NK, Mankar N, Nikhade PP, Chandak M. Beyond tradition: non-surgical endodontics and vital pulp therapy as a dynamic combination. *Cureus* 2023;15:e44134.
6. Thibodeau B, Teixeira F, Yamauchi M, Caplan DJ, Trope M. Pulp revascularization of immature dog teeth with apical periodontitis. *J Endod* 2007;33:680–9.
7. Aguilar P, Linsuwanont P. Vital pulp therapy in vital permanent teeth with cariously exposed pulp: a systematic review. *J Endod* 2011;37:581–7.
8. Diogenes A, Ruparel NB, Shiloah Y, Hargreaves KM. Regenerative endodontics: a way forward. *J Am Dent Assoc* 2016;147:372–80.
9. American Association of Endodontists. *AAE clinical considerations for a regenerative procedure*. Chicago: AAE, 2016.
10. Jeeruphan T, Jantarat J, Yanpiset K, Suwannapan L, Khewsawai P, Hargreaves KM. Mahidol study 1: comparison of radiographic and survival outcomes of immature teeth treated with either regenerative endodontic or apexification methods: a retrospective study. *J Endod* 2012;38:1330–6.
11. Lopes LB, Neves JA, Botelho J, Machado V, Mendes JJ. Regenerative endodontic procedures: an umbrella review. *Int J Environ Res Publ Health* 2021;18:754.
12. Wei X, Yang M, Yue L, et al. Expert consensus on regenerative endodontic procedures. *Int J Oral Sci* 2022;14:55.
13. Liang C, Liao L, Tian W. Stem cell-based dental pulp regeneration: insights from signaling pathways. *Stem Cell Rev Rep* 2021;17:1251–63.
14. Atila D, Chen CY, Lin CP, et al. *In vitro* evaluation of injectable tideglusib-loaded hyaluronic acid hydrogels incorporated with RG1-loaded chitosan microspheres for vital pulp regeneration. *Carbohydr Polym* 2022;278:118976.
15. Huang CC, Narayanan R, Alapati S, Ravindran S. Exosomes as biomimetic tools for stem cell differentiation: applications in dental pulp tissue regeneration. *Biomaterials* 2016;111:103–15.
16. Hammouda DA, Mansour AM, Saeed MA, Zaher AR, Grawish ME. Stem cell-derived exosomes for dentin-pulp complex regeneration: a mini-review. *Restor Dent Endod* 2023;48:e20.
17. Li Y, Liu C, Han G. Research progress of odontogenic extracellular vesicles in regeneration of dental pulp. *Oral Dis* 2023;29:2565–77.
18. Ganesh V, Seol D, Gomez-Contreras PC, Keen HL, Shin K, Martin JA. Exosome-based cell homing and angiogenic differentiation for dental pulp regeneration. *Int J Mol Sci* 2022;24:466.
19. Carter P, Bhattarai N. Engineered biomimicry. In: *Bioscaffolds: fabrication and performance*. Elsevier, 2013.

20. Li Z, Chu D, Gao Y, et al. Biomimicry, biomineralization, and bioregeneration of bone using advanced three-dimensional fibrous hydroxyapatite scaffold. *Mater Today Adv* 2019;3:100014.
21. Ng JY, Obuobi S, Chua ML, et al. Biomimicry of microbial polysaccharide hydrogels for tissue engineering and regenerative medicine—a review. *Carbohydr Polym* 2020;241:116345.
22. Guo X, Li J, Wu Y, Xu L. Recent advancements in hydrogels as novel tissue engineering scaffolds for dental pulp regeneration. *Int J Biol Macromol* 2024;264:130708.
23. Swarup S, Rao A, Suprabha B. Pulp regeneration using nano-hydroxyapatite as scaffold in an immature central incisor: a 10-month follow-up. *J Interdiscip Dent* 2014;4:89—92.
24. Liu H, Lu J, Jiang Q, et al. Biomaterial scaffolds for clinical procedures in endodontic regeneration. *Bioact Mater* 2022;12: 257—77.
25. Shahi S, Dehghani F, Abdolahinia ED, et al. Effect of gelatinous spongy scaffold containing nano-hydroxyapatite on the induction of odontogenic activity of dental pulp stem cells. *J King Saud Univ Sci* 2022;34:102340.
26. Sharifi S, Shahi S, Khalilov R, Dizaj SM, Abdolahinia ED. Gelatin—hydroxyapatite fibrous nanocomposite for regenerative dentistry and bone tissue engineering. *Open Dent J* 2022;16: e1874—2106.2022.0001.
27. dos Santos AC, dos Santos GG, Miguel FB, Cirelli JA, Rosa FP. Hydroxyapatite, alginate and gelatin composites used for bone regeneration: a systematic review. *Res Soc Dev* 2023;12: e14112340566.
28. Lestari W, Irfanita N, Haris MS, et al. Advancements and applications of gelatin-based scaffolds in dental engineering: a narrative review. *Odontology* 2025 (in press).